YAW ANGLE CONTROL FOR AUTONOMOUS VEHICLE USING KALMAN FILTER BASED DISTURBANCE OBSERVER

Binh Minh Nguyen [1)] Hiroshi Fujimoto [1)] Yoichi Hori [1)]

1) The University of Tokyo, Graduate School of Frontier Sciences, Department of Advanced Energy
5-1-5 Kashiwanoha, Kashiwa, Chiba, 277-8561, Japan
(E-mail: minh@hori.k.u-tokyo.ac.jp, fujimoto@k.u-tokyo.ac.jp, hori@k.u-tokyo.ac.jp)

Presented at the EVTeC and APE Japan on May 22, 2014

ABSTRACT: Yaw angle control is an essential function in every autonomous vehicle system. In this paper, a novel yaw angle control method for vehicle is proposed. Because the attitude of vehicle obtained from on-board GPS receiver is not only delayed but also at low rate in comparison with the control frequency of EPS servo drives, it is impossible to use GPS directly in yaw angle control loop. By integrating a single antenna GPS receiver with a yaw rate sensor using proposed Kalman filter, GPS measurement delay is handled and yaw angle is estimated at high rate. In order to improve the robustness of yaw angle control, disturbance observer utilizing estimated yaw angle and nominal yaw dynamics is designed. The disturbance observer serves as the inner-loop of the outer one with feedback-feed forward controllers. Simulations and experiments are performed to verify the proposed control system.

KEY WORDS: yaw angle control, GPS, course angle, Kalman filter, disturbance observer.

1. Introduction

In recent years, autonomous vehicle technology has been developed drastically to improve the safety and comfort of human's transportation. Besides the famous Google car, a number of works on autonomous driving can be found from literature review [(1~5)]. However, almost the previous works focus on navigation and guidance algorithm, such as position estimation or path planning. In contrast, less consideration is given to autonomous driving from the view point of dynamic motion control. In the autonomous vehicle system, the guidance layer outputs the attitude command, often represented by yaw angle, and velocity command. Therefore, yaw angle control plays an essential task in autonomous driving. Its function is to change the attitude of the vehicle to track with a desired path generated by the guidance layer. From this analysis, the following two problems are still challenges in yaw angle control design.

Problem 1: Yaw angle estimation: In low cost autonomous vehicle, course angle measured from GPS receiver can be used as the feedback of vehicle attitude [(6~7)]. However, course angle is not actually yaw angle, but yaw angle plus body sideslip angle. Moreover, data from GPS receiver is not always stable and at low update rate. The update rate of GPS receiver is from 1 Hz to 50 Hz which is much slower than the control frequency of the EPS motor drives which serve as actuators of yaw angle control (1 kHz or even more). Thus, using only GPS receiver surely limits the performance of yaw angle control. Yaw angle can also be calculated directly by using double-antenna GPS receiver, and then, the rate of yaw angle estimation can be improved by fusing GPS signal with that from inertial measurement unit (IMU) [(8)]. This method seems to be perfect, but, transparently, increases the cost and the complexity of the system. An affordable method is integrating single-antenna GPS receiver with yaw rate sensor based on linear bicycle model of vehicle [(9)]. However, this method is not robust enough under model uncertainties, and time delay of GPS signal is not considered. To improve this estimation scheme, we proposed to use "disturbance accommodating" in which augmented states stand for the influence of model uncertainties and external disturbances [(10)]. To deal with delayed measurement, we also proposed "pseudo-measurement" to construct a non-delayed measurement sequence. This method is successfully applied in visual servo system considering the delay of camera image processor [(11)]. In this paper, we propose to combine both "disturbance accommodating" and "pseudo-measurement" for estimating yaw angle.

Problem 2: Robustness of yaw angle control: In previous works, yaw angle control is often realized by simple feedback controller like PD or PID [(12~13)]. The robust issue of yaw angle control under the variation of road condition and the influence of disturbance as lateral wind force is not thoroughly examined. Considering this problem, we aim to improve the robustness by utilizing disturbance observer (DOB) [(14)]. In our control strategy, front steering angle generated by EPS servo motor is used as control input. The nominal yaw model which is independent of cornering stiffness is proposed for DOB design. Yaw angle tracking is achieved by combining a feedback with a feed forward controller as outer loop of DOB. Simulations and experiments are conducted to validate the effectiveness of the proposed control scheme.

2. Experimental Vehicle and Modeling

2.1. Experimental Vehicle

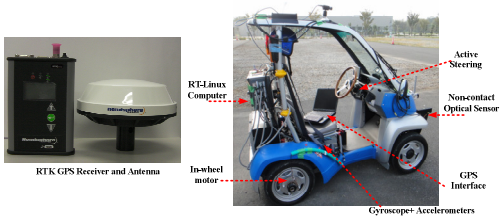

Fig. 1. Experimental EV and GPS receiver.

A one seat micro EV as shown in Fig. 1 is used for this study. It has two rear in-wheel motors and front EPS which is applicable for autonomous driving. Yaw rate sensor and accelerometers are installed at the center of gravity (CG) of the EV. Encoders are used for obtaining the rotational velocity of wheels and rotational angle of steering column. Vehicle control unit with RT-Linux operating system is used to implement the control algorithm. The basic sampling of the control system is 1 millisecond. A single-antenna GPS receiver, the Hemisphere R320, is used to provide vehicle position, velocity, and course angle with the maximum update rate of 20 Hz. The accuracy of vehicle positioning can reach 1 centimeter level when using the real-time kinematic mode (RTK) with paid correction signal.

2.2. Modeling of Yaw Motion

Planar bicycle model is used to model the dynamic of vehicle motion (Fig. 2). In this model, course angle v is the angle between vehicle direction and the geodetic North. It equals yaw angle ψ plus sideslip angle β, and can be obtained from GPS receiver. The following state space model is established:

$$\begin{cases} \dot{x} = Ax + Bu \\ y = Cx \end{cases} \tag{1}$$

$$x = \begin{bmatrix} \beta & \gamma & \psi \end{bmatrix}^T,\ u = \delta_f,\ y = \begin{bmatrix} \gamma & v \end{bmatrix}^T \tag{2}$$

$$A = \begin{bmatrix} a_{11} & a_{12} & 0 \\ a_{21} & a_{22} & 0 \\ 0 & 1 & 0 \end{bmatrix},\ B = \begin{bmatrix} b_{11} \\ b_{21} \\ 0 \end{bmatrix},\ C = \begin{bmatrix} 0 & 1 & 0 \\ 1 & 0 & 1 \end{bmatrix} \tag{3}$$

$$\begin{aligned} a_{11} &= -\frac{2\left(C_f + C_r\right)}{mu_x},\ a_{12} = -1 - \frac{2\left(C_f l_f - C_r l_r\right)}{mu_x^2} \\ a_{21} &= -\frac{2\left(C_f l_f - C_r l_r\right)}{I_z},\ a_{22} = -\frac{2\left(C_f l_f^2 + C_r l_r^2\right)}{I_z u_x} \\ b_{11} &= \frac{2C_f}{mu_x},\ b_{21} = \frac{2C_f l_f}{mu_x} \end{aligned} \tag{4}$$

where δ_f is the front steering angle, γ is the yaw rate, u_x is the longitudinal velocity, m is total mass of vehicle, l_f and l_r are the distances from CG to the front and rear axle of wheels, C_f and C_r are the cornering stiffnesses of the front and rear tires. From (1), the transfer function from front steering angle to yaw angle is derived as:

$$P(s) = \frac{\psi(s)}{\delta_f(s)} = \frac{b_{21}s + \left(a_{21}b_{11} - a_{11}b_{21}\right)}{s^3 + \left(-a_{11} - a_{22}\right)s^2 + \left(a_{11}a_{22} - a_{12}a_{21}\right)s} \tag{5}$$

In the planar coordinates, point O is the instantaneous rolling center of the vehicle. It is the intersection of lines AO and BO

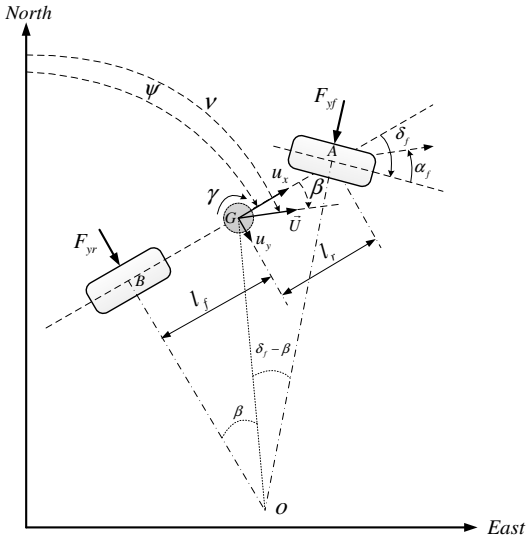

Fig. 2. Planar bicycle model.

which are perpendicular to the orientation of the front and rear rolling wheels. OC is the instantaneous radius of vehicle path. Apply the sine rule to the triangles OGA and OGB, the following relationships are derived:

$$\begin{cases} \tan\left(\delta_f\right)\cos\left(\beta\right) - \sin\left(\beta\right) = \dfrac{l_f}{OG} \\ \sin\left(\beta\right) = \dfrac{l_r}{OG} \end{cases} \tag{6}$$

Adding two equations in (6) together:

$$\tan\left(\delta_f\right)\cos\left(\beta\right) = \frac{l_f + l_r}{OG} \tag{7}$$

Assuming that vehicle velocity is almost constant and the radius of vehicle path does not change quickly, the rate of change of orientation of the vehicle would be equal to the angular velocity of the vehicle. We can write:

$$\dot{\psi} \approx \frac{u}{OG} = \frac{u\cos\left(\beta\right)}{l_f + l_r}\tan\left(\delta_f\right) \tag{8}$$

Assuming that the front steering angle is small, the final relationship between the rate of yaw angle and front steering angle is obtained as:

$$\dot{\psi} \approx \frac{u_x}{l_f + l_r}\delta_f \tag{9}$$

3. Design of Yaw Angle Control System

The block diagram of the yaw angle control system is shown in Fig. 3. In the following sub-sections, we will explain the design of this proposed system.

3.1. Yaw Angle Reference

Autonomous navigation can be classified into three strategies: Point-to-point, path following, and trajectory tracking [15]. Among them, point-to-point navigation is the simplest way such that the

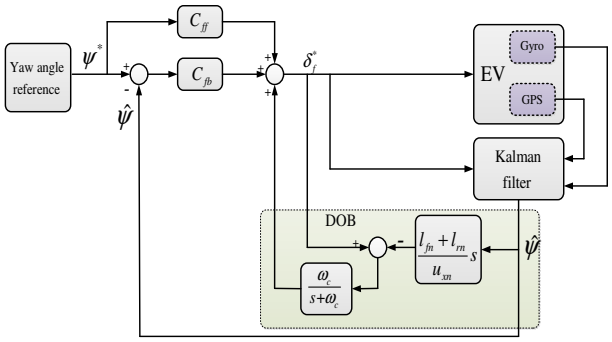

Fig. 3. Block diagram of yaw angle control system.

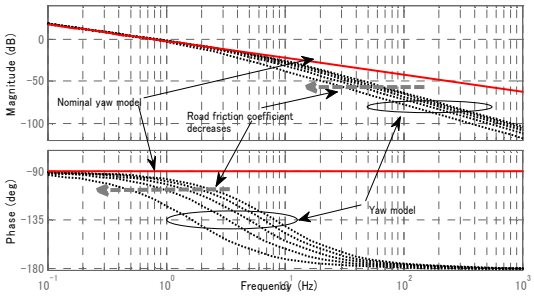

Fig. 4. Bode diagram of nominal and parameter variation model.

desired yaw angle to navigate the vehicle from point A_1 (x_1, y_1) to point A_2 (x_2, y_2) is calculated as:

$$\psi^* = \begin{cases} \tan^{-1}\left(\dfrac{x_2 - x_1}{y_2 - y_1}\right) & (y_2 > y_1) \\ \pi - \tan^{-1}\left(\dfrac{x_2 - x_1}{y_2 - y_1}\right) & (y_2 < y_1, x_2 > x_1) \\ \tan^{-1}\left(\dfrac{x_2 - x_1}{y_2 - y_1}\right) - \pi & (y_2 < y_1, x_2 < x_1) \end{cases} \tag{10}$$

A long path can be divided into number of segments, for instance, A_1A_2, A_2A_3, …, $A_{n-1}A_n$. In each segment, yaw angle reference is kept constant.

3.2. Yaw Angle Estimation

There are two problems to be solved in yaw angle estimation design. Firstly, the variation of tire cornering stiffness according to road surface condition may degrade the estimation accuracy. Secondly, while the yaw rate's sampling time is the same as control period (1 ms), the sampling time of course angle is much longer. Moreover, course angle is possible delayed as explained in the Introduction.

To solve the first problem, we proposed to use disturbance accommodating Kalman filter in which the extended states represent the influence of model uncertainties and external disturbances [10]. The dynamics of extended system is expressed as follow (in discrete-time):

$$\begin{bmatrix} x_{k+1} \\ d_{k+1} \end{bmatrix} = \begin{bmatrix} A_{d,k} & I \\ 0 & I \end{bmatrix} \begin{bmatrix} x_k \\ d_k \end{bmatrix} + \begin{bmatrix} B_{d,k} & 0 \\ 0 & I \end{bmatrix} \begin{bmatrix} u_k \\ r_{d,k} \end{bmatrix} + \begin{bmatrix} w_k \\ w_{d,k} \end{bmatrix} \tag{11}$$

where d_k is the extended state which is assumed to be random walk process with rate $r_{d,k}$. w_k and $w_{d,k}$ are the process noises which are assumed to have Gaussian distribution with zero mean.

To solve the second problem, we proposed "pseudo-measurement" to construct the non-delayed measurement sequence and fulfill the inter-samples [11] (the samples between two consecutive updates of course angle). Assume that at sample k, a course angle measurement is updated. However, it is delayed N samples. Until the next update of course angle, the pseudo-measurement vector is calculated as follows:

$$\begin{cases} y^* = \begin{bmatrix} \gamma_k + \eta_{\gamma,k} \\ \hat{v}_{k+i|k+i-1} + G_{k+i}\left(v_k - \hat{v}_{k-N|k-N-1}\right) \end{bmatrix} \\ v_k = \psi_{k-N} + \beta_{k-N} + \eta_{v,k-N} \end{cases} \tag{12}$$

where G_{k+i} (i = 0,1,2…) is an invertible gain matrix to calculate the pseudo course angle, $\hat{v}_{k+i|k+i-1}$ and $\hat{v}_{k-N|k-N-1}$ are the predicted course angles, $\eta_{\gamma,k}$ and $\eta_{d,k}$ are the measurement noises which are assumed to have Gaussian distribution with zero mean.

Due to the limitation of page numbers, Kalman filter algorithm with disturbance accommodating and pseudo-measurement is not shown in this paper. The detailed algorithms can be seen in previous publications of our group [10~11].

3.3. Disturbance Observer (DOB)

DOB was firstly introduced by Ohnishi [14] and then further refined by Hori's groups [16]. According to this method, the feedback loop includes a model of the dynamic of the exogenous reference and disturbance signal, called nominal internal model. By carefully designing the nominal model and a Q-filter, the perfect asymptotic tracking and disturbance compensation are achieved. Until now, DOB has been widely applied as a robust motion control method, especially in electric vehicles, such as lateral force observer and yaw moment observer [17].

As shown in the previous Section, the model of yaw angle dynamics contains cornering stiffnesses which are time-varying parameters. A controller which is designed using constant cornering stiffnesses would be not as robust enough as requirement. Of course, it is possible to indentify the cornering stiffness in real-time [18] and adaptive controller can be designed. However, the existence of parameter identification will increase the cost and the complexity of general system. It is also a non-trivial work to assure the robustness of control system with cornering stiffness identification. Moreover, the vehicle system is interfered by unknown disturbances such as lateral wind force. In this paper, to improve the robustness of yaw angle control, DOB is applied. From (9), the nominal internal model is designed as follows:

$$P_n(s) = \frac{u_x}{(l_f + l_r)s} = \frac{k_n}{s} \tag{13}$$

The nominal model does not rely on tire cornering stiffness, but velocity and vehicle geometric distances. Bode diagram in Fig. 4 is to compare the yaw dynamics in (5) with the nominal yaw dynamics. This diagram is plotted at the velocity of 25 kph and tire cornering stiffnesses are varied in range of 2000 N/rad to 7000 N/rad (or from low friction road to high friction road). The yaw model can be expressed as nominal model with multiplicative perturbation as model uncertainties:

$$P(s) = P_n(s)\left[1 + \Delta(s)\right] \tag{14}$$

where $\Delta(s)$ is a proper boundary and stable transfer function representing the model uncertainties.

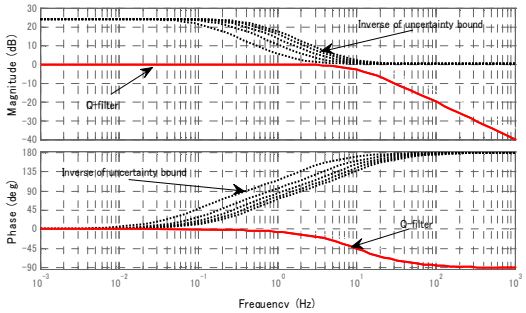

Fig. 5. Q-filter design for DOB at velocity of 25 kph.

The model uncertainty transfer function is calculated as:

$$\Delta(s) = \frac{P(s) - P_n(s)}{P_n(s)} \tag{15}$$

Generally, both disturbance and model uncertainties are regarded as equivalent disturbance in DOB. The DOB is designed to compensate the equivalent disturbance, and the inner-loop is forced to be approximately nominal model. Robust stability of inner-loop is assured if Q-filter satisfies the following condition for all frequencies:

$$\left|Q(j\omega)\right| < \frac{1}{\left|\Delta(j\omega)\right|} \tag{16}$$

Because the nominal model is first order, Q-filter is selected as a first order low-pass-filter:

$$Q(s) = \frac{\omega_c}{s + \omega_c} \tag{17}$$

The cut-off frequency of Q-filter is selected as 20 Hz in this paper. Fig. 5 shows that when changing the tire cornering stiffnesses, the magnitude of Q-filter is always bounded by magnitude of the inverse of uncertainty transfer function. In other words, the robust stability condition is satisfied.

3.4. Feedback and Feed Forward Controller

The feedback and feed forward controllers make up the outer-loop of the yaw angle control system. The feed forward one is simply designed as the inverse of the nominal model:

$$C_{ff}(s) = \frac{1}{k_n} s \tag{18}$$

PI controller is selected as feedback controller such that two poles of the close loop can be placed arbitrarily. Noticing that the inner-loop with DOB can be approximately nominal transfer function, the gains of the PI controller are computed as:

$$\begin{cases} C_{fb}(s) = k_p + \dfrac{k_i}{s} \\ k_p = -\dfrac{(s_1 + s_2)}{k_n} \\ k_i = \dfrac{s_1 s_2}{k_n} \end{cases} \tag{19}$$

where s_1 and s_2 are two desired poles of the close-loop.

4. Verification of Proposed Yaw Angle Control System

4.1. Yaw Angle Estimation-Experimental Results

Experiment results of yaw angle estimation. Course angle from RTK-GPS receiver's sampling time is 200 ms (5 Hz update rate), and it is intentionally delayed 100 ms. It is to simulate the signal obtained from conventional low-cost GPS receiver. Model uncertainties are introduced into the estimation model such that real cornering stiffness of vehicle model is equal to 80% of the cornering stiffness of estimation model. The delay of and low rate of measured course angle is shown in Fig. 6 (a), in comparison with the measured course angle. Thanks to the "pseudo-measurement", estimated yaw angle converses to true yaw angle, as in Fig. 6 (b). Notice that, the measured yaw angle is obtained from Corrsys Datron's sideslip angle sensor and RTK-GPS whose costs are very expensive. Sideslip angle estimation results are demonstrated in Fig. 6 (c), by comparing the proposed method with linear observer using yaw rate and lateral acceleration sensors [19]. Thanks to the disturbance accommodating, better sideslip angle estimation is achieved with the proposed method.

4.2. Yaw Angle Control-Simulation Results

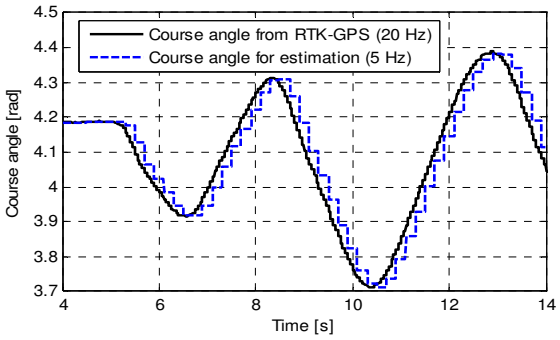

(a) Course angle.

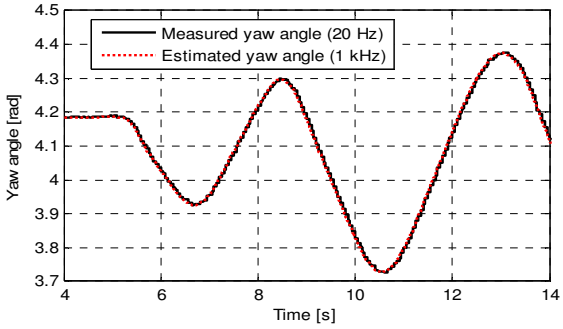

(b) Yaw angle estimation.

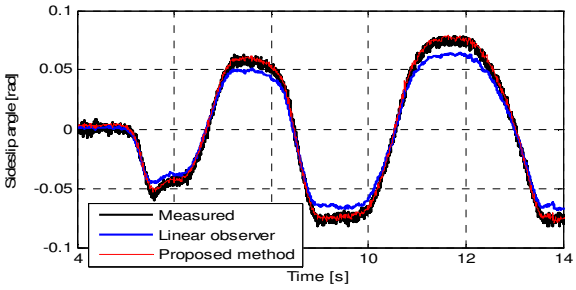

(c) Sideslip angle estimation.

Fig. 6. Estimation results (experiment).

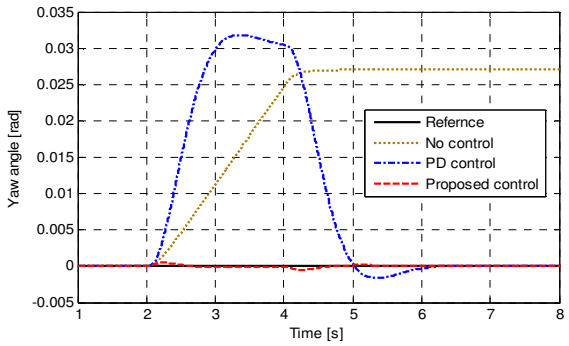

(a) Yaw angle.

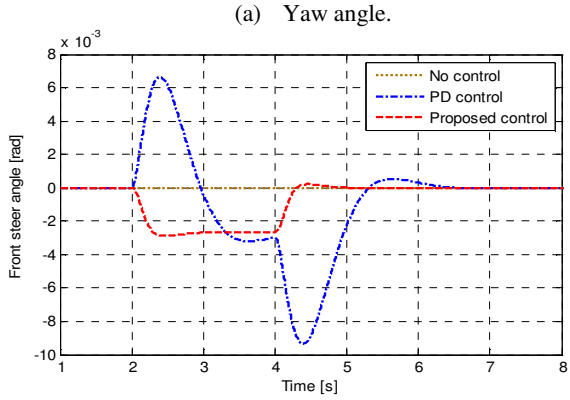

(b) Front steering angle.

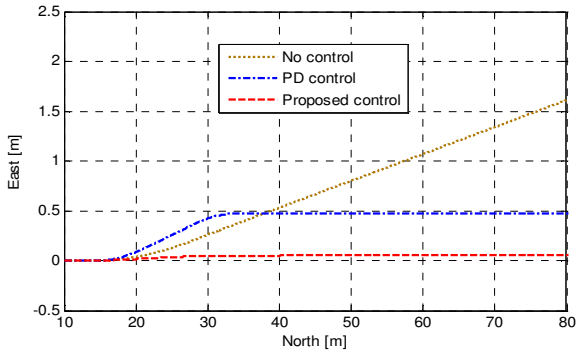

(c) Vehicle trajectory.

Fig. 7. Yaw angle control results (simulation).

As explained in the previous Section, path planning can be divided into number of segments. In each segment, yaw angle reference is constant. Therefore, keeping constant yaw angle is the very basic task to verify firstly. In the simulation, vehicle velocity is 25 kph, and vehicle is desired to keep zero yaw angle. In other words, the motion of vehicle is straightforward to the North. Strong lateral wind force starts to interfere the vehicle since 2 second. The conventional system with feed forward and feedback controllers (PD) are performed for comparison. In conventional system, PD controller is designed based on pole placement using the transfer function of yaw dynamics expressed in (5) which relies on tire cornering stiffness. C_f and C_r are cornering stiffnesses of vehicle model, while C_{fn} and C_{rn} are cornering stiffnesses for control design. To verify the robust issue, model uncertainties are set such that $C_f / C_{fn} = C_r / C_{rn} = 0.8$.

Simulation results are summarized as follows: Fig. 7 (a) illustrates the responses of vehicle yaw angle according to different control schemes; Fig. 7(b) performs the front steering angles which are the control inputs; Fig. 7 (c) expresses the trajectories of vehicle motion. In case of without control, the front steering angle is always zero. As a result, the vehicle cannot follow the straightforward direction into North due to the influence of wind force. If the conventional control scheme is applied, it takes a long time for the vehicle to recover the desired direction. Thanks to the proposed scheme with DOB, the disturbance is suppressed and model uncertainties are compensated. Consequently, the vehicle can quickly recover the reference yaw angle. Moreover, the lateral position error of the proposed scheme is considerably reduced in comparison with that of conventional scheme.

4.3. Yaw Angle Control-Experimental Results

To evaluate the proposed yaw angle control scheme, we conduct the autonomous driving test. In the first experiment, the vehicle trajectory is desired to be parallel with the direction of the test course. Yaw angle reference is pre-calculated by using formulation (10). A “virtual disturbance” is generated by program to verify the robust issue. All the results including yaw angle response, front steering angle, and vehicle trajectories are shown in Fig. 8. In case of without control, the front EPS motor always keeps zero front steering angle. Therefore, the yaw angle and trajectory of vehicle cannot follow the references. In contrast, when applying the proposed control scheme, the front steering angle is generated to compensate the influence of disturbances. As a result, the tracking of yaw angle and trajectory are successfully achieved.

In another test, the vehicle is desired to, firstly, go straight, and then, make a cornering (Fig. 9). In case of without control, yaw angle tracking is impossible because front steering command is just generated as pre-decided. When applying the proposed control scheme, again, tracking performance is done.

5. Conclusion

In this paper, a new yaw angle control method for autonomous driving of vehicle is proposed. The control scheme is designed based on the following contributions: 1) Yaw angle is estimated by a low cost configuration consisting of a single-antenna GPS receiver and yaw rate sensor. Yaw angle is estimated at high rate considering the uncertainties of estimation model and the delay of course angle from GPS receiver. 2) As the author’s understanding, this is the first time such that disturbance observer (DOB) is applied to improve the robustness of yaw angle control. Based on the analysis of yaw motion, the nominal model is designed such that it does not rely on tire cornering stiffnesses which are time-varying parameters which is hardly to know exactly in real-time. In this paper, the pattern of vehicle trajectory is still simple. In future work, we will conduct autonomous driving test with more complicated trajectory.

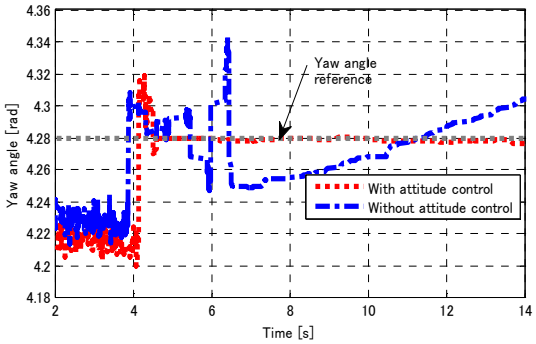

(a) Yaw angle.

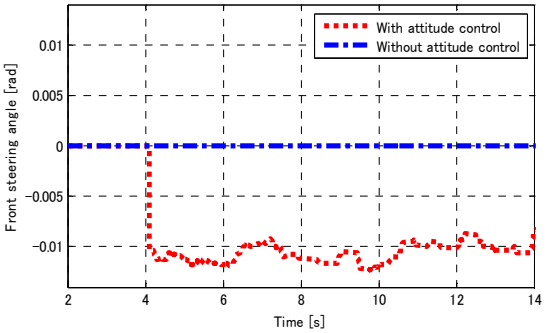

(b) Front steering angle.

(c) Vehicle trajectory (without control)

(d) Vehicle trajectory (with control)

Fig. 8. Yaw angle control results (experiment).

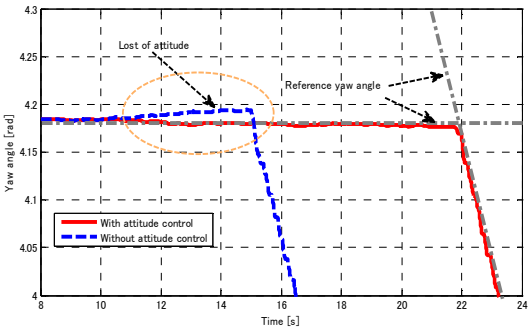

(a) Yaw angle.

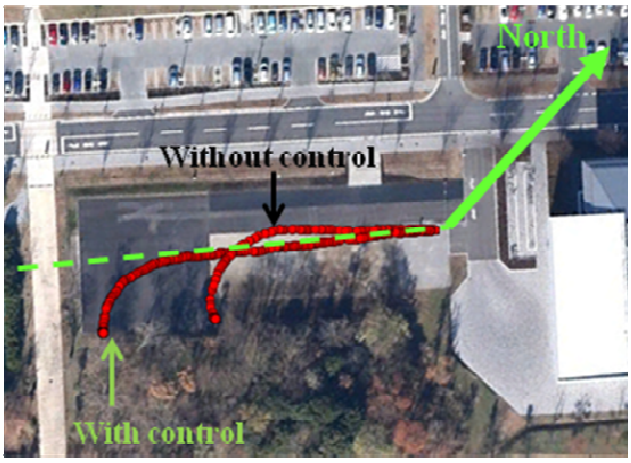

(b) Vehicle trajectory.

Fig. 9. Autonomous driving test (experiment).

References

(1) S. Suzuki : Autonomous Navigation, Guidance and Control of Small 4-wheel Electric Vehicle, Journal of Asian Electric Vehicles, Vol. 10, No. 1, p.1575-1582 (2012).

(2) J. Connors and G. H. Elkaim : Trajectory Generation and Control Methodology for an Autonomous Ground Vehicle, AIAA Guidance, Navigation, and Control Conference and Exhibit, Vol. 8, p.5704-5722 (2008).

(3) G. V. Raffo, G. K. Gomes, J. E. Normey-Rico, C. R. Kelber, and L. B. Becker : A predictive Controller for Autonomous Vehicle Path Tracking, IEEE Transactions on Intelligent Transportation System, Vol. 10, No. 1, p. 92-102 (2009).

(4) J. Kang, R. Y. Hindiyeh, S. W. Moon, J. C. Gerdes, and K. Yi : Design and Testing of a Controller for Autonomous Vehicle Path Tracking Using GPS/INS Sensors, 17th World Congress-The International Federation of Automatic Control, p. 2093-2098 (2008).

(5) T. Keviczky, P. Kalcone, F. Borrelli, J. Asgari, and D. Hrovat : Predictive Control Approach to Autonomous Vehicle Steering, Proceedings of the 2006 American Control Conference, p.4670-4675 (2006).

(6) R. W. Wall, J. Bennett, and G. Eis : Creating a Low-cost Autonomous Vehicle, Proceedings of 28th Annual Conference of the Industrial Electronics Society, Vol. 4, p.3112-3116 (2002).

(7) M. E. Holden : Low-Cost Autonomous Vehicles Using Just GPS, Proceedings of the 2004 American Socirty for Engineering Education Annual Conference & Exposition (2004).

(8) D. M. Bevly, J. Ryu, and J. C. Gerdes : Integrating INS Sensors with GPS Measurements for Continuous Estimation of Vehicle Sideslip, Roll, and Tire Cornering Stiffness, IEEE Transactions on Intelligent Transportation System, Vol. 7, No. 4, p.483-493 (2006).

(9) R. Anderson and D. M. Bevly : Using GPS with a Model-Based Estimator to Estimate Critical Vehicle States, Vehicle System Dynamics, Vol. 48, No. 12, p.1413-1438 (2010).

(10) B. M. Nguyen, Y. Wang, H. Fujimoto, and Y. Hori：Lateral Stability Control of Electric Vehicle Based on Disturbance Accommodating Kalman Filter using the Integration of Single Antenna GPS Receiver and Yaw Rate Sensor, Journal of Electrical Engineering Technology, Vol. 8, No. 4, p.899-910 (2013).
(11) B. M. Nguyen, K. Ito, W. Ohnishi, Y. Wang, H. Fujimoto, Y. Hori, M. Odai, H. Ogawa, E. Takano, T. Inoue, and M. Koyama：Dual Rate Kalman Filter Considering Delayed Measurement and Its Application in Visual Servo, Proceedings of 13th International Workshop on Advanced Motion Control (2014).
(12) W. Travis and D. M. Bevly：Trajectory Duplication Using Relative Position Information for Automated Ground Vehicle Convoys, Proceedings of IEEE Position, Location and Navigation Symposium, p.1022-1032 (2008).
(13) H. Suppachai, C. Silawatchananai, M. Parnichkun, and C. Wuthishungwong：Double Loop Controller Design for the Vehicle's Heading Control, Proceedings of the 2009 IEEE International Conference on Robotics and Biometrics, p.989-994 (2009).
(14) K. Ohnishi：A New Servo Method in Mechatronics, Transactions of Japanese Society of Electrical Engineers, Vol. 107-D, p.83-86 (1987).
(15) A. D. Luca and G. Oriolo：Feedback Control of a Nonholonomic Car-like Robot, Chapter 4 of Planning Robot Motion, J. P. Laumond Ed., Springer-Verlag (1997).
(16) T. Umeno and Y. Hori：Robust Speed Control of DC Servomotors Using Modern Two Degrees-of-Freedom Controller Design, IEEE Transactions on Industrial Electronics, Vol. 38, No. 5, p.363-368 (1991).
(17) H. Fujimoto and Y. Yamauchi：Advanced Motion Control of Electric Vehicle Based on Lateral Force Observer with Active Steering, Proceedings of IEEE International Symposium on Industrial Electronics, p.3627-3632 (2010).
(18) H. Fujimoto, N. Takahashi, A. Tsumasaka, and T. Noguchi：Motion Control of Electric Vehicle Based on Cornering Stiffness Estimation with Yaw-Moment Observer, Proceedings of 9th International Workshop on Advanced Motion Control, p.206-211 (2006).
(17) H. Fujimoto and Y. Yamauchi：Advanced Motion Control of Electric Vehicle Based on Lateral Force Observer with Active Steering, Proceedings of IEEE International Symposium on Industrial Electronics, p.3627-3632 (2010).
(19) Y. Aoki, T. Uchida, and Y. Hori：Experimental Demonstration of Body Slip Angle Control Based on a Novel Linear Observer for Electric Vehicle, Proceedings of 31st Annual Conference of IEEE Industrial Electronics Society, p.2620-2625 (2005).